P. Siegmann, L. Felipe-Sesé, F.A. Díaz, An alternative approach for improving DIC by using out-of-plane displacement information, Optics and Lasers in Engineering, Volume 128, 2020, 105996, ISSN 0143-8166, https://doi.org/10.1016/j.optlaseng.2019.105996.

An alternative approach for improving DIC by using out-of-plane displacement information

P. Siegmann[a], L. Felipe-Sesé[b], F.A. Díaz[b]

[a] Departamento de Teoría de la Señal y Comunicaciones, Universidad de Alcalá, 28805 - Alcalá de Henares, Spain. Email: philip.siegmann@uah.es

[b] Departamento de Ingeniería Mecánica y Minera, Campus las Lagunillas, Universidad de Jaén, 23071 - Jaén, Spain. Email: {lfelipe, fdiaz}@ujaen.es

Abstract

A new approach to perform 2D Digital Image Correlation (DIC) on objects that are subjected to large out-of-plane displacements is presented. It employs out-of-plane information to distort the speckle images of the reference and the deformed surface, increasing their similarity and therefore their sub-set cross-correlation peaks. The new approach is implemented using the combined Fringe Projection and 2D-DIC technique on two experiments: The buckling of an initial flat plate, and the rotation of the reference surface towards the camera from 0º to 60º. In both cases large speckle distortions are produced due to two issues, the lens magnification and the surface tilting. The first speckle distortion is applied to the deformed image to perform the lens magnification correction, and the second speckle distortion is applied to the reference image. The obtained distorted speckle images become very similar, allowing to successfully compute corresponding pixels between both images in a simple way (i.e. without nonlinear minimization processes). For this propose, an analytical iterative equation is derived to determine pixel displacements due to out-of-plane surface tilting. The resulting displacements are compared with those obtained by the conventional procedure, applying 2D-DIC (using open source Ncorr software) on the non-distorted speckle images and then making the lens magnification correction. The novel procedure proposed makes it possible to successfully find the corresponding pixels at the reference surface for out-of-plane rotations of 55º and 60º for which Ncorr failed. 3D-DIC (using commercial VIC software) is also employed to validate the results.

Keywords: Digital image correlation; fringe projection; displacement maps, speckle image distortion.

1 Introduction

The precise determination of large 3D displacement maps is still an issue when the deformation of the object happens too fast for the camera to acquire images in short intervals, or if they can not be acquired during the deformation process, like in stamping processes. Commonly, 3D Digital Image Correlation (3D-DIC) is used to measure large 3D deformations, but it requires two synchronized cameras and an expensive software [1]. A single colour camera can also be used in addition with two mirrors and a X-cube prism or a dichroic filter to combine two views from different perspectives [2,3]. The present work proposes an alternative way which is economic and simple, based on an improved technique that combines Fringe Projection and 2D-DIC (FP+2D-DIC). In particular, it is intended to improve the DIC procedure of samples subjected to large 3D deformations. Therefore, before entering into detail, a short overview of DIC is given next to give the necessary background knowledge and nomenclature used throughout the manuscript.

Digital image correlation allows to determine the displacements of the pixels between two speckle images of the same surface before and after being deformed. A pixel at (x_1, y_1) of the speckle image before being deformed, $\mathbf{I}_1$, is surrounded by a unique speckle pattern within a subset that can be recognized in the image of the deformed speckle pattern, $\mathbf{I}_2$, centered at the location (x_2, y_2), by finding the maximum of the cross correlation between the subsets of both speckle images. The notation here used for the DIC operation applied on two speckle images, $\mathbf{I}_1$ and $\mathbf{I}_2$, to provide the in-plane displacement maps of each pixel in the region of interest of $\mathbf{I}_1$ is

$$\left[\Delta x_{12}(x_1, y_1), \Delta y_{12}(x_1, y_1)\right] = \text{DIC}\left[\mathbf{I}_1(x_1, y_1), \mathbf{I}_2(x_2, y_2)\right]. \tag{1}$$

One important factor in the accuracy of the computed displacements, (Δx_{12}, Δy_{12})=(x_2-x_1, y_2-y_1), is the amount of distortion of the speckle pattern when the surface is deformed. It is common to us nonlinear minimization approach of a cost function that takes into account subset distortions to improve the cross-correlation between the subsets and considerably improving the determination of the displacements with subpixel resolution [1]. For example, the 2D-DIC open source algorithm "Ncorr" uses the Gauss-Newton iterative optimization scheme, a biquintic B-spline interpolation and follows a reliability guided path along pixels with the highest cross correlation (letting the pixels with lower correlation values to be processed last) to further improve the accuracy in the determination of the pixel displacements [4,5]. Nonetheless, large rotation of the surface can still produce errors. An improved DIC for large in-plane rotations has already been proposed in [6], in the present work it is proposed a way for dealing with large out-of-plane rotations.

In the present work, it is proposed an alternative way to improve DIC results for surfaces with displacements in the three spatial directions, by using the information of out-of-plane displacements to remove speckle distortion due to *lens magnification* and to *surface tilting* effects. It will be shown how to determine the in-plane displacements caused by these effects and how to use them to accordingly change the speckle images, $\mathbf{I}_1$ and $\mathbf{I}_2$, to make them more similar. In this way, it is possible to increase the cross correlation peaks between corresponding subsets, or even allow to find the peaks if they were not (i.e. in the case of very large out-of-plane inclination).

The information of the out-of-plane displacement can be obtained, for instance, from the projected fringes in the combined FP+2D-DIC technique [7-9]. In this case FP provides the out-of-plane displacements (or z-displacements) for all the pixels in the region of interest of the image $\mathbf{I}_2$ of the deformed surface, while the in-plane displacements (in x- and y-direction) are provided by 2D-DIC. For simplicity, it is assumed an initial flat surface (z_1=0) and after deformation, each pixel of the surface will have an out-of-plane displacement of Δz.

Two experiments are shown, a plate that is bent to obtain a large slope change and a flat surface that is rotated from 0 to 60 deg. around an axis perpendicular to the optical axis. The new proposed processing method is then compared with the open source software Ncorr and with 3D-DIC which uses the commercial software VIC3D from Correlated Solutions Inc [1].

2 Experimental set-up

The experimental set-up is shown in Fig. 1(a), where, as example of deformation, an initial flat plate is subjected to a compression load to generate buckling. The white plate is painted with a red speckle pattern and illuminated under a certain inclination with blue and white fringes using a Dell M115HD WXGA 1280x800 projector. A color digital camera "0" observes the specimen surface (shown in Fig. 1(b)) with its optical axis perpendicular to the initial flat reference surface. Camera "1" and "2" (model Stingray F-080C 1/3 with 25 mm lens) are alternatively used with camera "0" to perform 3D-DIC from two different points of view, with a pan angle between them of 30º. For 3D-DIC the commercial software VIC-3D is employed. Camera "0" is a 3CCD camera, model JAY AT-200GE, where the R, G and B images are obtained with their respective CCD matrix, and a 25 mm lens. Two images are acquired to compute the 3D displacement maps, one of the initial flat reference surface and the other one after applying the load. As in [3], the 3CCD camera allows a very good separation of the information provided by the different channels, in our case the speckle information from the fringe information. The B-channel sees only the speckle (since the blue fringes are not appreciated when seen through the blue filter of the 3CCD camera) while the R-channel sees the fringes (since the red speckle are not appreciated when seen through the red filter), separating in this way both information's with very low cross talk as shown in Fig. 1(c) and (d). Nonetheless, some residual high frequency noise from the speckle in the fringe images can be appreciated and smoothed away with a low pass filter. The fringe images are used to compute the out-of-plane displacement map (in *z*-direction) while the speckle images provide the in-plane displacement maps (in *x*- and *y*-direction).

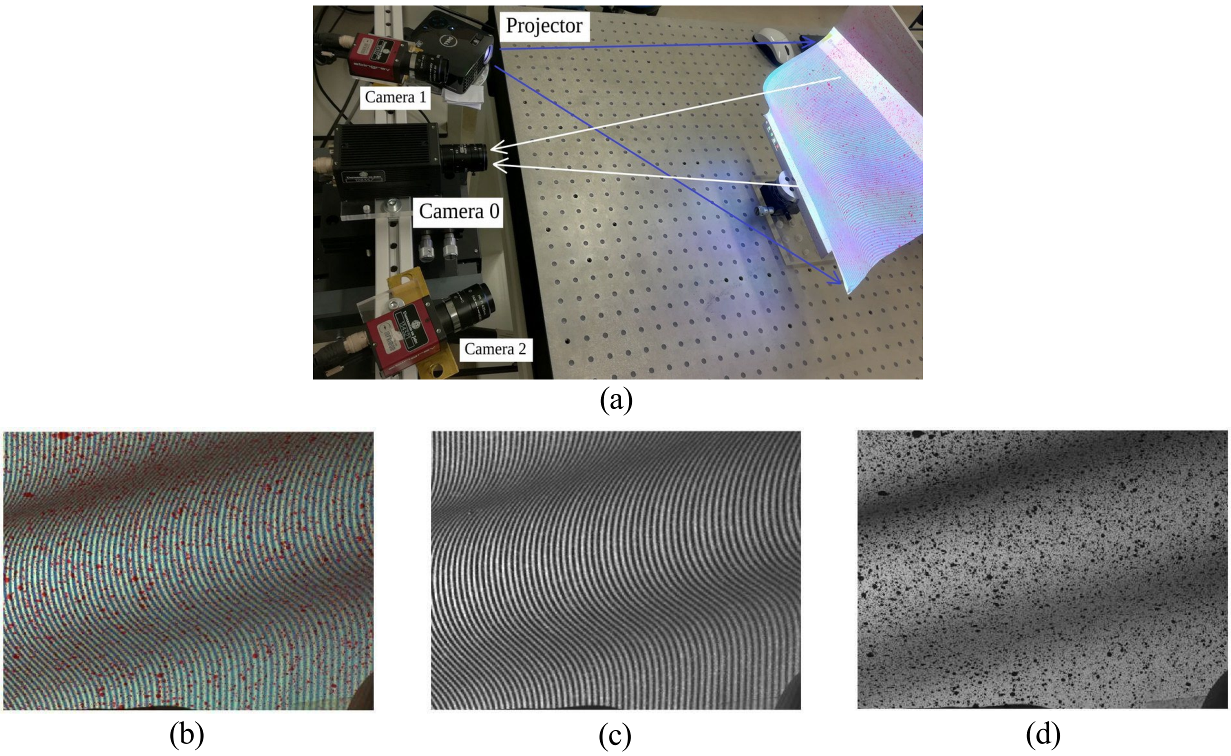

Fig. 1. (a) Experimental set-up. (b) Acquired RGB image with Camera 0. (c) R-channel image. (d) B-channel image.

The z-displacements, Δz, are obtained from the fringe images using for example the procedure proposed in [9] for large z-displacements and for fringes projected in a divergent way. At each pixel of the region of interest (ROI), the shifted phase is obtained from the shifted fringe using, for instance, the adaptive asynchronous algorithm proposed in [10] (which only requires the reference and the deformed fringe images). The shifted (and unwrapped) phase, ϕ, is then related to the corresponding out-of-plane displacement, Δz, through a 2nd order polynomial, $\Delta z = p_1\phi + p_2\phi^2$, where p_1 and p_2 are two calibration parameters obtained for each pixel. The calibration consist then on acquiring a set of known Δz values and the corresponding ϕ values, and performing a 2nd order polynomial fitting from which p_1 and p_2 are obtained. In the present case, 11 images of the reference fringe image placed at z_0 +(-30, -25, -20, -15, -10, 0, 10, 15, 20, 25, 30) mm, were acquired, being z_0 the distance relative to the camera from which the z-displacements are measured. This distance, and the center of the image (x_v, y_v), is obtained from the slope and vertex of so called "cone of radial displacement", which is obtained experimentally from the absolute value of the radial displacement map between pixels of the reference plane placed at z_0 and at, for instance, z_0 + 25 mm.

From the Δz map the direction of the maximum tilting angle, θ (azimuth angle), and the tilting angles, β (polar angle), of each surface element can be obtained. These angles will be required to perform one of the proposed speckle image distortion, and they are obtained from the x- and y-gradients of Δz, g_x and g_y, as follows:

$$\begin{cases} \theta = \frac{\pi}{2} - \arctan \frac{g_x}{g_y}, \\ \beta = \arctan \sqrt{g_x^2 + g_y^2} \end{cases} \quad (2)$$

The gradient makes the noise to be amplified, therefore a previous "severe" smoothing of Δz has to be done. The proposed smoothing process is done as follows. A drastic size reduction of the Δz map (e.g. from 480×640 pixels to equidistantly distributed 30×40 pixels) is performed using a linear interpolation fitting to obtain a smooth but down resized Δz map. Values of the fitted function only exist at these reduced number of pixels and therefore the final smoothed Δz map is obtained by resizing it up to its initial size (from 30×40 to 480×640) using a nearest-neighbor interpolation method. Fig. 2 shows the Δz map before and after being smoothed. In this way, the partial derivatives for computing the polar and azimuth angles are effectively smoothed, as shown in Fig. 3 for a profile of the polar angle along the y-axis. On the same figure, it is also shown the corresponding result when applying a median filter with a neighborhood window of 100×100 pixels on the original Δz map, which gives unacceptable fluctuating results.

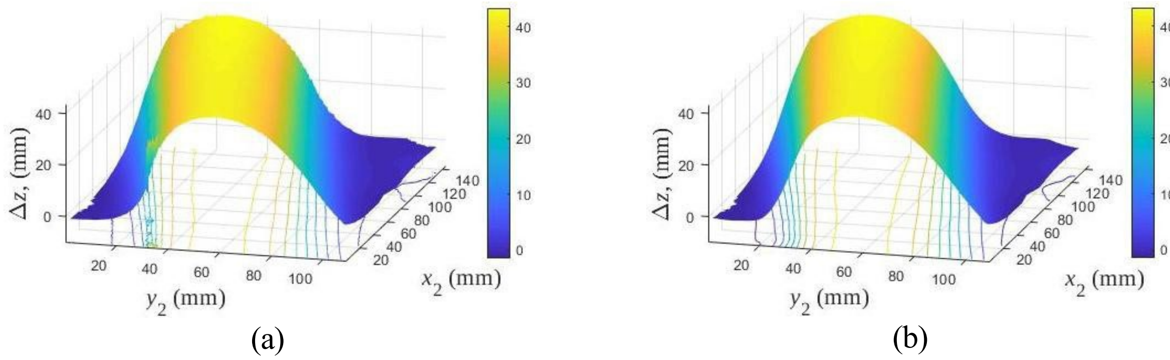

Fig. 2. (a) Δz map. (b) Smoothed Δz map.

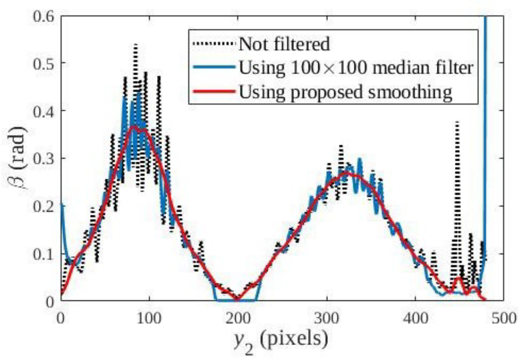

Fig. 3. Profile of the polar angle estimation obtained from the corresponding z-map's as an example of the performance of the proposed smoothing process.

3 Proposed procedure

In this section, only the main idea of the proposed alternative procedure for improving DIC using out-of-plane displacement information in comparison to the conventional procedure is explained. The detailed procedure is explained in the following section. As shown on the flow diagram of the Fig. 4, both procedures starts with the two initial speckle images, the reference, $\mathbf{I}_1$, and the deformed, $\mathbf{I}_2$, one. The traditional way of processing these two images is by directly applying DIC on them to obtain the in-plane displacements (Δx_{12}, Δy_{12}), with abbreviated nomenclature Δ_{12}, where sub-indices "12" stands for reference "1" to the corresponding deformed "2" pixel position. But Δ_{12} may be affected by the lens magnification effect if there has been out-of-plane displacements. This effect is then corrected by applying the corresponding correction to Δ_{12} to finally obtain the in-plane displacements Δ_{1m}, where sub-indice "m" stands for "magnification" corrected deformed pixel position.

The proposed way performs this lens magnification correction previous to applying DIC. The speckle displacements caused by the lens magnification effect is used to conveniently distort the deformed speckle image, $\mathbf{I}_2$, obtaining the magnification corrected one, $\mathbf{I}_m$. In this way, part of the speckle distortion between $\mathbf{I}_1$ and $\mathbf{I}_2$ is eliminated, making $\mathbf{I}_m$ more similar to $\mathbf{I}_1$ than $\mathbf{I}_2$. Herewith DIC between $\mathbf{I}_1$ and $\mathbf{I}_m$ is improved and provides the in-plane displacements without lens magnification effect.

The DIC can further be improved by estimating the speckle distortion caused by the tilting effect. In this case the reference speckle image, $\mathbf{I}_1$, is distorted to obtain a "projected" speckle image, $\mathbf{I}_p$. This distortion is performed by displacing the pixels of $\mathbf{I}_1$ the known distances Δ_{1p}, which will be calculated in the next section. The distorted speckle image, $\mathbf{I}_p$, becomes even more similar to $\mathbf{I}_m$, increasing their cross correlation values of corresponding pixels and further improving DIC. Nonetheless, to the obtained in-plane displacements, Δ_{pm}=DIC[$\mathbf{I}_p$, $\mathbf{I}_m$], the known distances Δ_{1p} have to be added to obtain the displacements Δ_{1m}.

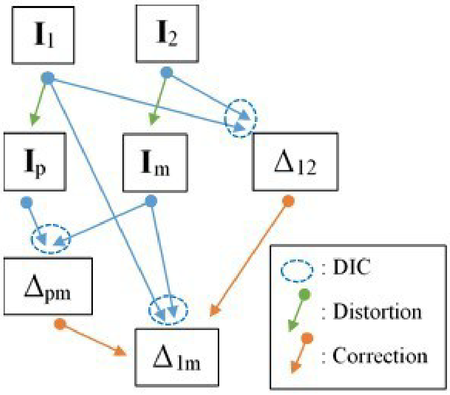

Fig. 4. Flow diagram. $\mathbf{I}_p$ and $\mathbf{I}_m$ are the distorted speckle images of $\mathbf{I}_1$ and $\mathbf{I}_2$, respectively. Δ_{12}=DIC[$\mathbf{I}_1$, $\mathbf{I}_2$], Δ_{pm}=DIC[$\mathbf{I}_p$, $\mathbf{I}_m$] and Δ_{1m}=DIC[$\mathbf{I}_1$, $\mathbf{I}_m$]. Δ_{1m} is the final in-plane displacement, while Δ_{12} and Δ_{pm} have to be corrected by respectively subtracting and adding the required correction displacements.

4 Speckle image distortion due to Δz

The distortion of the speckle images due to out-of-plane displacements requires to know first the corresponding in-plane displacements of the pixels due to *z*-displacements of the visualized surface. Thus, in-plane displacements are a consequence of two distinguishable causes, the lens magnification (if no telecentric lens is used) and the specimen surface out-of-plane inclination or tilting. The displacement due to the tilting is calculated for the pixels of the reference speckle image (obtaining with them the distorted reference speckle image), and the displacements due to magnification effect is calculated for the pixels of the deformed speckle images (obtaining the distorted deformed speckle image, which is then without lens magnification). The final in-plane displacement map is then obtained by adding the displacements used to obtain the distorted reference image, with the displacement obtained by applying DIC between the distorted reference speckle images and the distorted deformed speckle image.

4.1 In-plane displacement due to Δz

For an initial flat specimen surface, the lens magnification causes the image of a surface element to displace in radial direction (in *x*- and *y*-direction) with respect to the optical axis of the camera (*z*-axis) when the surface element is displaced in *z*-direction as it is shown in Fig. 5, where the surface element at position 1 moves to position 2 without varying the distance, *h*, from the optical axis (OA). This displacement causes the image of the element surface of each pixel of the image of the deformed speckle surface, $\mathbf{I}_2$, to be displaced the amount:

$$\begin{cases} C_x(x_2, y_2) = (x_2 - x_v)\dfrac{\Delta z(x_2, y_2)}{z_0}, \\ C_y(x_2, y_2) = (y_2 - y_v)\dfrac{\Delta z(x_2, y_2)}{z_0}, \end{cases} \tag{3}$$

where z_0 is the distance between the camera and the flat reference surface, (x_v, y_v) the center of the image (trough which crosses the OA) and considering Δz positive if moving towards the camera and negative otherwise [7]. In the reported experiment z_0 = 513 mm, (x_v, y_v) = (352, 228) pixels, and the lateral magnification L=0.227 mm/pixels [8]. The corrected displacement that each pixel in $\mathbf{I}_2$ has experimented due to the deformation of the specimen is then

$$\begin{cases} \Delta x_{12,C}(x_2, y_2) = \Delta x_{12}(x_2, y_2) - C_x, \\ \Delta y_{12,C}(x_2, y_2) = \Delta y_{12}(x_2, y_2) - C_y, \end{cases} \tag{4}$$

where the sub-indices "12" refers to the displacement from pixel in $\mathbf{I}_1$ to corresponding pixel in $\mathbf{I}_2$.

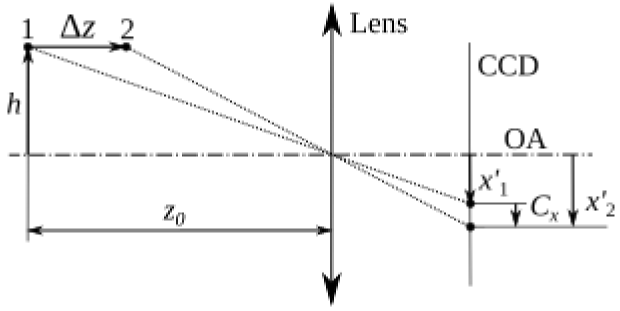

Fig. 5. Scheme of the displacement measured at the CCD (from x'_1 to x'_2) due to the out-of-plane displacement Δz. OA is the optical axis. ($x'_2 = x_2 - x_v$).

The tilting of the surface will also produce pixel displacements due to the perspective change. In a first approach, it is considered only one-dimensional slope change, i.e., changes in the inclination of straight surface stripes of the specimen as shown in Fig. 6, where a thin flat plate is buckled as a result of a compression load, F.

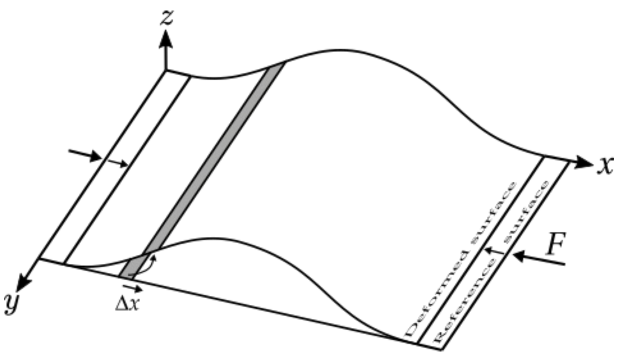

Fig. 6. Plate subjected to a compression load which produces an in-plane displacement of the stripes depending on the amount of the out-of-plane displacement.

It will be shown how to determine the in-plane displacements (Δx) of the surface stripes from the information of the out-of-plane displacements (i.e. known the direction at which the surface element displaces and its maximum slope value). This will be done by wrapping the reference speckle image around the known contour of the deformed surface. For this propose an initial wrapping stripe in $\mathbf{I}_1$ is selected at the position in $\mathbf{I}_2$ with the highest value of Δz (Fig. 7). Since the pixels along this initial stripe should not displace in x- and y-direction, a rigid body displacement of the speckle image $\mathbf{I}_1$ is performed by displacing the whole image a distance that makes the in-plane displacement of the pixel belonging to the initial stripe to be zero:

$$\mathbf{I}_r(x_r, y_r)=\mathbf{I}_1(x_1-\Delta x_{1r}, y_1-\Delta y_{1r}), \tag{5}$$

The rigid body displacement is performed by attaching empty pixels to the image $\mathbf{I}_1$ to the corresponding side increasing it the amount (Δx_{1r}, Δy_{1r}). These displacements are obtained by a simple cross correlation (CRC) between image $\mathbf{I}_1$ and $\mathbf{I}_2$ of a small subset around any pixel (x_{ini},y_{ini}) belonging to the initial stripe in $\mathbf{I}_2$,

$$(\Delta x_{1r},\Delta y_{1r})=\mathrm{CRC}\left[\mathbf{I}_2,\mathbf{I}_1,(x_{ini}, y_{ini})\right]. \tag{6}$$

where the sub-indices "1r" refers to the displacements of the pixels from $\mathbf{I}_1$ to $\mathbf{I}_r$. Fig. 7 illustrates this procedure. Also the smoothed Δz map is increased with empty pixels at the opposite side as $\mathbf{I}_r$ to make their size equal. This slip is necessary for the following wrapping process.

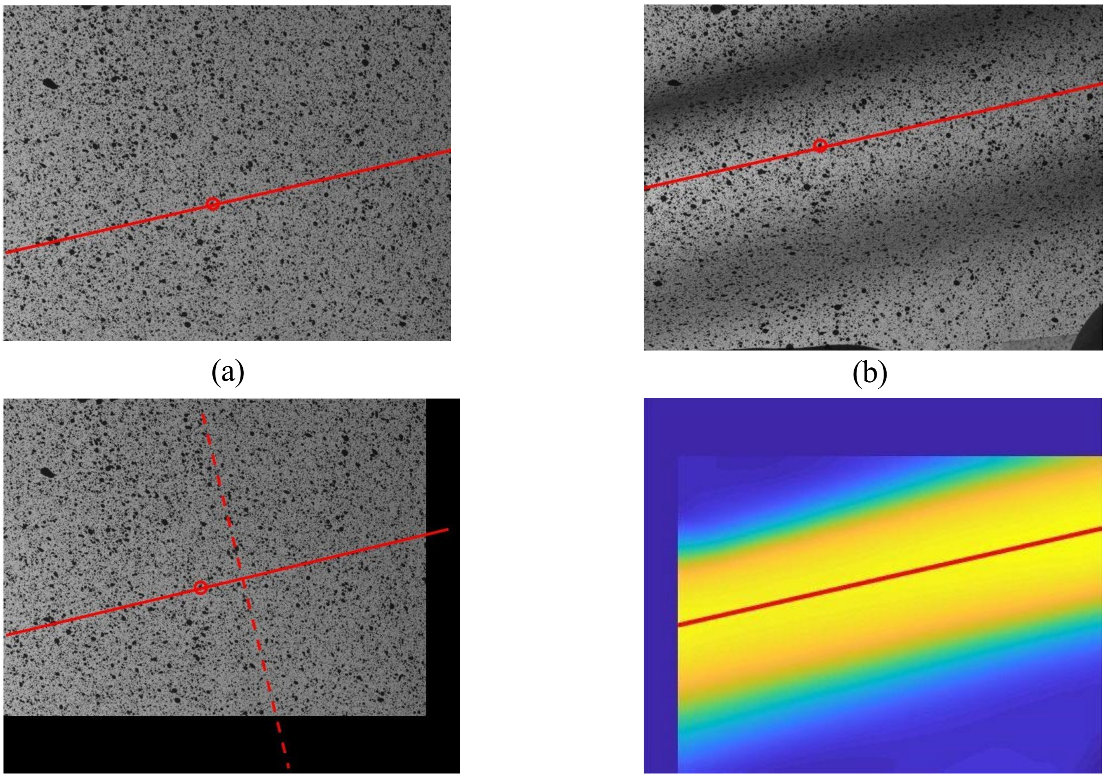

Fig. 7. (a) Reference speckle image, $\mathbf{I}_1$, and, (b) deformed speckle image, $\mathbf{I}_2$, with initial strip marked with a red continuous line. (c) Rigid-body translated reference image $\mathbf{I}_r$, to place the initial stripe at the position with highest value of the smoothed Δz map shown in (d). Red circle marks an (x_{ini}, y_{ini}) pixel with highest Δz value used to make the CRC.

After this rigid body displacement, Fig. 8 shows, a scheme to estimate the pixel displacement produced by the wrapping process. A black continuous line shows a simplified example of a portion (a few pixels) of a deformed surface profile. The borders of the stripes are designed with i=1,2,... and k=1,2,.., which are respectively the positions of the pixels of the images $\mathbf{I}_r$ and $\mathbf{I}_2$ of the reference and deformed surface. In this simplified example the surface is compressed along the x-axis, producing the corresponding known z-displacements of each stripe. Before deformation, the surface stripes visualized by the pixels of the camera are regularly distributed along the flat specimen surface separated a distance l. After z-deformation, the pixel images corresponds to different stripes of the surface due to the in-plane displacement. The amount of displacement of each stripe can be obtained by consecutively projecting them from the flat surface onto the deformed surface *maintaining their relative distances* l, and starting from the stripe (i=k=1) with highest z-value who have not displaced, $\Delta x_{T,i=1}=0$. The following stripes moves in x-direction towards it the amount:

$$\Delta x_{T,i}=\sum_{j=1}^{i-1}\Delta x_j+\Delta x_i \text{ for } i=2,3,\ldots \tag{7}$$

where the x-displacements of the previous (already displaced) surface stripe are added to the following pixels to be projected, being the displacement due to the tilting of just the i^{th} surface stripe segment:

$$\Delta x_i=l\left(1-\cos\alpha_i\right). \tag{8}$$

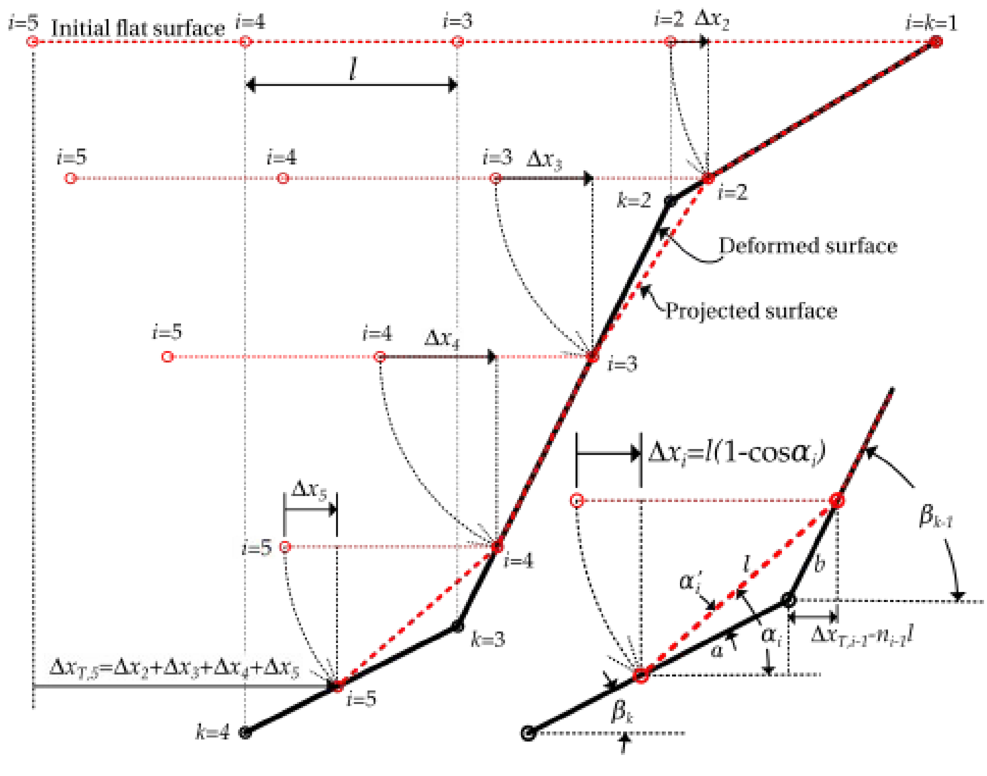

Fig. 8. To determine the in-plane displacements, the segments of the flat surface (discontinuous red line) are consecutively projected over the deformed surface (black continuous line). These projections produce the Δx_i displacements. A scheme of the involved geometrical parameters to determine Δx_i is shown at the bottom right.

If the projected segment falls entirely on the segment of the deformed surface (as happens with i=4 in Fig. 8) then the angle of inclination of the i^{th} projected segment, α_i, coincides with the angle of the slope of the k^{th} segment of the deformed surface, $\alpha_i=\beta_k$, being $k=i-n_{i-1}$, and n_i the entire number of times the displacement of the surface stripe, $\Delta x_{T,i}$, overpasses the distance l, (i.e. $n=n_i$ is updated when $\Delta x_{T,i} > (n_{i-1}+1)l$, then $n_i = n_{i-1}+1$, else $n_i = n_{i-1}$). Else, if the projected segment falls on a new segment of the deformed surface (as happens for example for i=5), then

$$\alpha_i=\beta_k - s\cdot\alpha'_i=\beta_k - s\cdot\arccos\frac{a^2+l^2-b^2}{2al}, \tag{9}$$

where $s=\mathrm{sign}(\beta_k-\beta_{k-1})$, and a,b are the sides of the triangle a-b-l that forms the projected segment with the segments of the deformed surface (shown in Fig. 8 bottom-right), which are

$$\begin{cases} a=-b\cos(\beta_k-\beta_{k-1})+\sqrt{l^2-(b\sin(\beta_k-\beta_{k-1}))^2}, \\ b=\dfrac{\Delta x_{T,i-1}-n_{i-1}l}{\cos\beta_{k-1}}. \end{cases} \tag{10}$$

It is then possible to iteratively calculate the in-plane displacement of each stripe for surfaces that have experimented non uniform out-of-plane displacement with the information of the slope of the deformed surface. However, only one dimensional slope change is considered in this approach.

The compression load, F, in Fig. 6 may be applied along any other direction within the (x,y)-plane, with an angle θ respect the x-axis. In this case the displacements of Eq. (7) are obtained along this direction, designed with ΔR_T instead of $\Delta x_{T,i}$, being the displacement of each individual segment as before $\Delta R_i=l_\theta(1-\cos\alpha_i)$, but with a different distance between segments, l_θ, that depends on the direction. These displacements are referred to pixels of strips along lines perpendicular to the direction of displacement. These lines with slope $\tan(\theta+\pi/2)$ are traced through consecutive pixels along the x-axis if the $|\tan(\theta+\pi/2)| \leq 1$ or, along the y-axis if $|\tan(\theta+\pi/2)|>1$. The distance l_θ is obtained from the distance between the parallel lines. And the x- and y-component of the pixel displacements of the pixels in the stripe along these lines is:

$$\begin{cases} \Delta x_{rp}=\Delta R_T\cos(\theta), \\ \Delta y_{rp}=\Delta R_T\sin(\theta), \end{cases} \tag{11}$$

where the sub-indices "rp" refers to displacements from rigid-body displaced pixel to projected pixel. The angle θ, gives the direction of the maximum slope (azimuth angle) and is obtained together with angle of inclination, β, in the direction of maximum slope (polar angle) for each pixel of the region of interest of the image of the deformed surface obtained from the smoothed Δz map using Eq. (2). Fig. 9 shows a cross section of the wrapping performed by the proposed process along the red discontinuous profile shown in Fig. 7(c). This wrapping does not need to be perfect, it is enough to obtain an approximated slope close to the real one to estimate the produced speckle distortion.

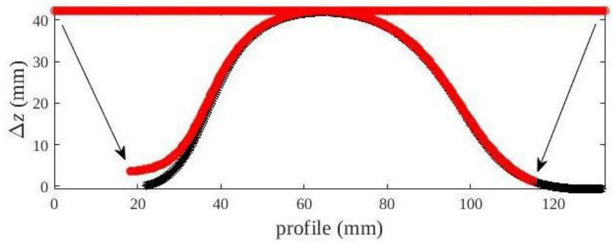

Fig. 9. Profile along the discontinuous red line shown in Fig. 7(c) of the projection of the rigid-body displaced reference speckle surface over the deformed surface (in black).

4.2 Distortion of the speckle images

Once the in-plane displacements of the pixels are known, this information can be used to accordingly distort the speckle images.

To remove the lens magnification effect, the pixel's intensities in $\mathbf{I}_2$ have to be displaced the distances given by Eq. (3). The distorted speckle image without magnification effect, $\mathbf{I}_m$, is obtained as follows:

$$\mathbf{I}_m(x_m, y_m) = W\left[\mathbf{I}_2(x_2, y_2), (C_x, C_y)\right], \tag{12}$$

using an operator W that performs a translation of the pixels information, in this case of $\mathbf{I}_2$, at (x_2, y_2) to the locations $(x_m, y_m) = (x_2 - C_x, y_2 - C_y)$ which may be no longer regularly distributed (in columns and rows) as (x_2, y_2). In W, an initially zero matrix of $\mathbf{I}_m$ of the same size as $\mathbf{I}_2$ is updated with the intensity values of the translated pixels. At this translated locations (x_m, y_m) the intensity value of $\mathbf{I}_2$ at (x_2, y_2) is supposed to have a Gaussian distribution, and is accordingly distributed between the $v \times v$ closest pixels (with v=4) as shown in the Appendix.

The distorted speckle image due to tilting is calculated from the initial flat reference speckle image subjected to rigid-body displacement, $\mathbf{I}_r$, obtained with Eq. (4). In this case the pixel at the initial flat surface (x_r, y_r) is displaced to the "projected" positions (x_p, y_p). The distorted speckle image, $\mathbf{I}_p$, can be determined by projecting the intensity of the pixels $\mathbf{I}_r$ over the corresponding displaced pixels in $\mathbf{I}_p$, using the operator W and the displacements of Eq. (11),

$$\mathbf{I}_p(x_p, y_p) = W\left[\mathbf{I}_r(x_r, y_r), (-\Delta x_{rp}, -\Delta y_{rp})\right]. \tag{13}$$

In this case W performs a translation of the pixel intensities of $\mathbf{I}_r$ at (x_r, y_r) to the locations $(x_p, y_p) = (x_r + \Delta x_{rp}, y_r + \Delta y_{rp})$. The speckle image $\mathbf{I}_p$ as well as the displacement maps Δx_{rp} and Δy_{rp} have the same size as $\mathbf{I}_r$ which was rigid body displaced by attaching empty pixels. $\mathbf{I}_p$, Δx_{rp} and Δy_{rp} have then to be resized to have the same original size as $\mathbf{I}_m$. Δx_{rp} and Δy_{rp} are resized by removing these pixels, and $\mathbf{I}_p$ is resized by removing the same number of pixels but from the opposite side. Fig. 10 shows the distorted speckle images, the resized one $\mathbf{I}_p$ and $\mathbf{I}_m$ obtained with Eq. (13) and (12) respectively. They have increased their similarity highlighting the cross correlation peak values when performing DIC.

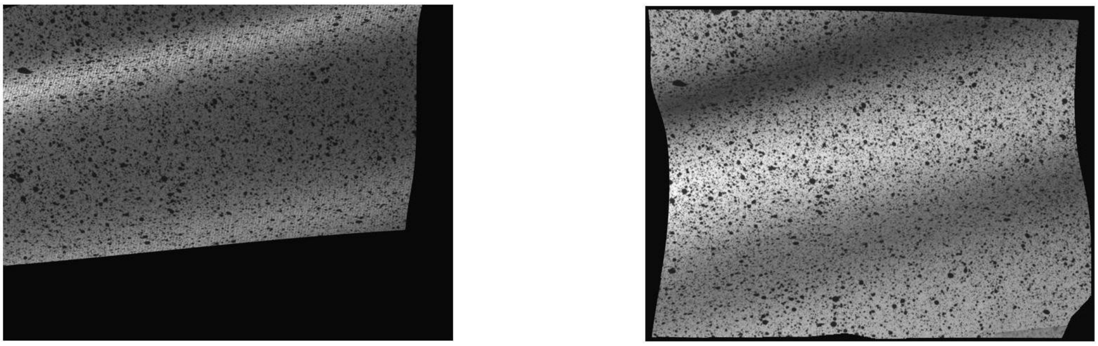

(a) (b)

Fig. 10. Distorted speckle images. (a) Projected speckle image, $\mathbf{I}_\mathrm{p}$. (b) Corrected deformed speckle image, $\mathbf{I}_\mathrm{m}$.

4.3 Corrected in-plane displacements

Finally, the remaining in-plane displacements is obtained from the distorted speckle images $\mathbf{I}_\mathrm{p}$ and the magnification corrected image $\mathbf{I}_\mathrm{m}$ using 2D-DIC,

$$[\Delta x_{\mathrm{pm}}, \Delta y_{\mathrm{pm}}] = \mathrm{DIC}[\mathbf{I}_\mathrm{p}, \mathbf{I}_\mathrm{m}]. \tag{14}$$

The displacements obtained with Eq. (14) are referred to the pixels of $\mathbf{I}_\mathrm{p}$, $(x_\mathrm{p}, y_\mathrm{p})$. The displacement experimented by each pixel of the initial speckle image without lens magnification can then be calculated by adding the previous induced displacements in the following way:

$$\begin{cases} \Delta x_{1\mathrm{m}}(x_1, y_1) = \Delta x_{1\mathrm{r}}(x_1, y_1) + \Delta x_{\mathrm{rp}}(x_1 + \Delta x_{1\mathrm{r}}, y_1 + \Delta x_{1\mathrm{r}}) \\ \qquad + \Delta x_{\mathrm{pm}}(x_1 + \Delta x_{1\mathrm{r}} + \Delta x_{\mathrm{rp}}, y_1 + \Delta y_{1\mathrm{r}} + \Delta y_{\mathrm{rp}}), \\ \Delta y_{1\mathrm{m}}(x_1, y_1) = \Delta y_{1\mathrm{r}}(x_1, y_1) + \Delta y_{\mathrm{rp}}(x_1 + \Delta x_{1\mathrm{r}}, y_1 + \Delta x_{1\mathrm{r}}) \\ \qquad + \Delta y_{\mathrm{pm}}(x_1 + \Delta x_{1\mathrm{r}} + \Delta x_{\mathrm{rp}}, y_1 + \Delta y_{1\mathrm{r}} + \Delta y_{\mathrm{rp}}), \end{cases} \tag{15}$$

where the total displacement of the pixel at (x_1, y_1) has to be tracked by localizing it on each displacement map.

As it will be shown, the in-plane displacements obtained in this way coincide with the one obtained using 2D-DIC directly on the reference and deformed speckle image and then subtracting the lens magnification effect (Eq. (4)), but again, referred to pixels of the reference image (x_1, y_1):

$$\begin{cases} \Delta x_{12,\mathrm{C}}(x_1, y_1) = \Delta x_{12,\mathrm{C}}(x_2 - C_x, y_2 - C_y), \\ \Delta y_{12,\mathrm{C}}(x_1, y_1) = \Delta y_{12,\mathrm{C}}(x_2 - C_x, y_2 - C_y). \end{cases} \tag{16}$$

The proposed procedure to obtain the in-plane displacement maps by conveniently distorting the reference and deformed speckle image allows to correctly find the corresponding pixel positions of speckle images from surfaces that have experienced large out-of-plane deformations. It is not even necessary to use the costly computational iterative nonlinear least squares optimization scheme to minimize the cross correlation function; it is enough to use the zero normalized cross correlation (zncc), with a reliability-guided path following algorithm and a quadratic surface fitting to the zncc values around its maximum to find, by its maximum, the corresponding subpixel position [5,11].

5 Experimental results and discussion

The in- and out-of-plane displacement maps of the buckled plate shown in Fig. 1, are obtained using FP+2D-DIC and 3D-DIC. For FP+2D-DIC camera "0" was used, and the cameras employed for 3D-DIC were camera "0" and "1", and also camera "0" and "2" (to have both perspectives). VIC software provides the displacement maps referred to the pixel positions of the reference speckle image, therefore, for comparison, the Δz map obtained using FP (shown in Fig. 2) has to be referred to the same pixel positions. These Δz maps are shown in Fig. 11. A difference is appreciated between the profiles shown in Fig. 11(d) which reaches ±2 mm at the highest point (about ±5% difference). 3D-DIC provides two different results depending on the set of cameras used, both are different from the one obtained with FP; one is over and the other below in about the same magnitude, therefore the result obtained with FP is probably closer to the real Δz displacement. When using 3D-DIC for large out-of-plane displacements, it is recommended to set-up a large angle between the cameras of about 60º as appointed on page 249 of [1]. In the reported experiment one of the cameras (the 3CCD camera) has to be perpendicular to the reference image, limiting the pan angle with the second camera on just about 30º. Therefore, this not big enough pan angle may lead to an error.

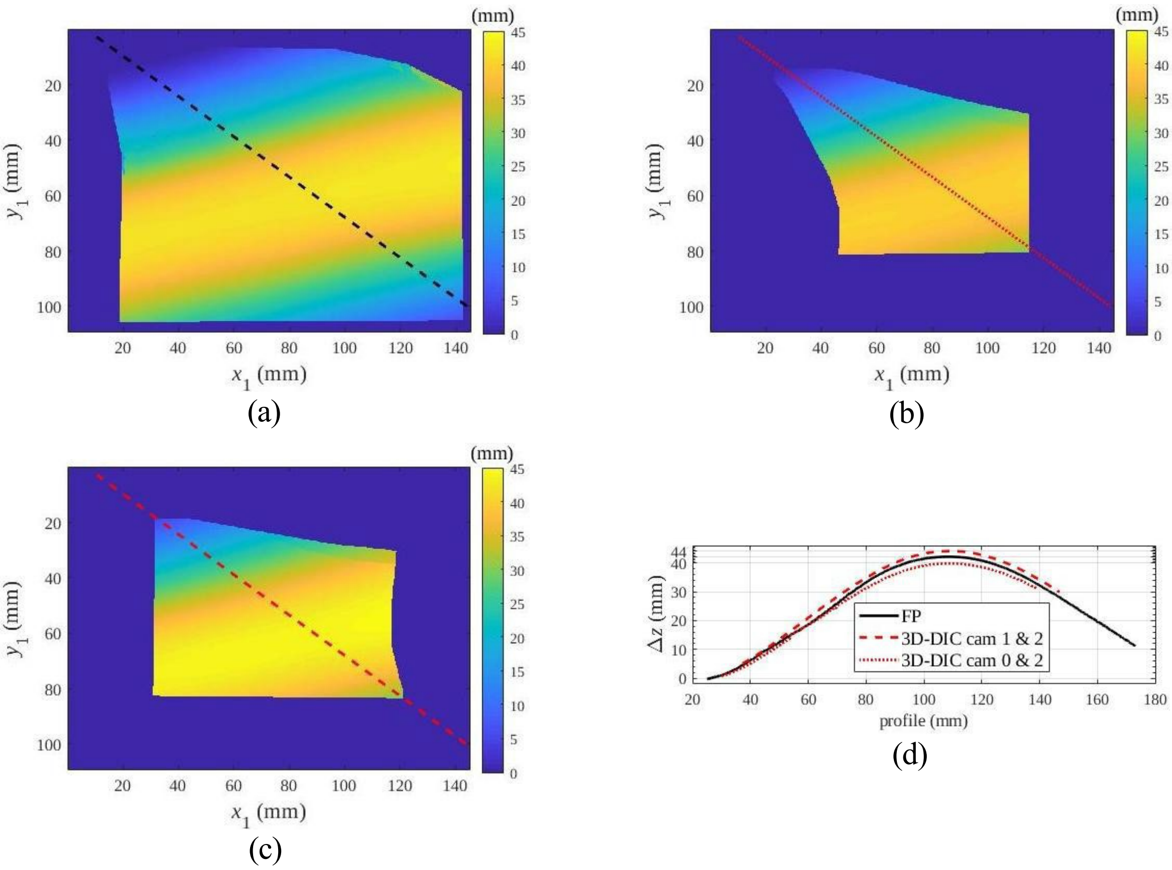

Fig. 11. Out-of-plane displacement maps referred to pixels of the reference image. (a) Obtained with FP, (b) and (c) obtained with 3D-DIC using respectively camera 0 and 2, and 0 and 1. (d) Profiles along the dashed lines shown on the respective Δz maps.

For the in-plane displacements the results obtained using FP+2D-DIC with the proposed speckle image distortion method (Eq. (15)) are compared with the one obtained using Ncorr software on images $\mathbf{I}_1$ and $\mathbf{I}_2$, and then making the lens magnification correction (Eq. (4) and (16)). In Fig. 12, the absolute value of the in-plane distance, $\Delta r = (\Delta x^2 + \Delta y^2)^{1/2}$, is shown. As it can be seen, both results coincide, being the root means square of the difference of both profiles shown in Fig. 10(d) (black continuous line and red dotted line) 0.033 mm and a mean percentage of difference of 0.2%. When comparing Δr obtained with the proposed method with the corresponding results obtained with 3D-DIC using cameras 0 and 1 (black continuous line and dashed blue line in Fig. 12(d)), a difference is again appreciated, of about 1.5 mm, at the zone of highest Δz displacements, between 80 mm and 140 mm along the profile, which corresponds to a difference of about 7%. As mentioned before, this error may be due to the not big enough pan angle used for 3D-DIC. On the whole, the root mean square of the difference of the profiles is 1.016 mm, with a mean percentage of difference of 5%.

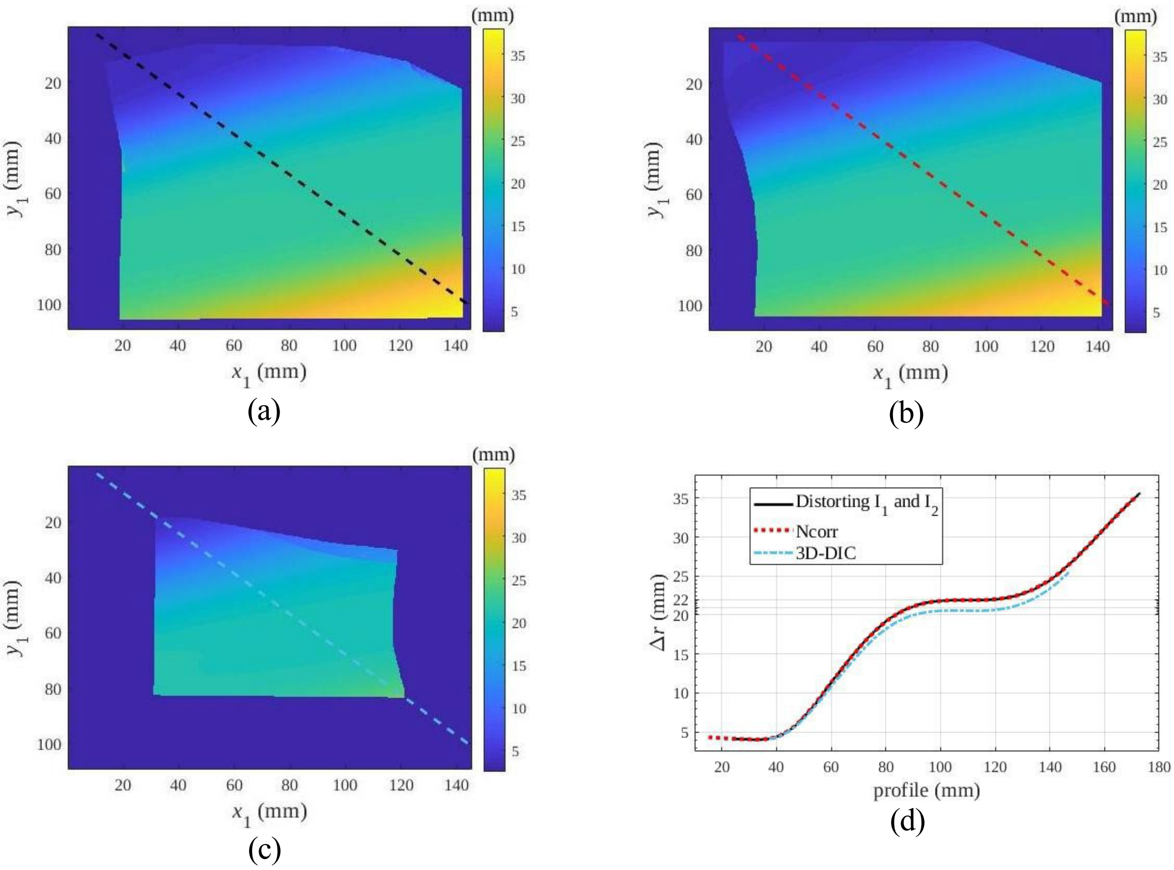

Fig. 12. Absolute value of the in-plane displacement map. (a) Obtained with the proposed method by distorting $\mathbf{I}_1$ and $\mathbf{I}_2$; (b) Obtained with Ncorr applied directly on $\mathbf{I}_1$ and $\mathbf{I}_2$; (c) obtained with 3D-DIC using cameras 0 and 1 and commercial VIC software. (d) Shows the corresponding profiles drawn in the respective maps.

Using the same set-up, another experiment has been done by rotating the reference surface several degrees (about 20º, 30º, 40º, 45º, 50º, 55º and 60º) around an axis parallel to the *y*-axis as shown in Fig. 13(a). For this experiment the rigid body displacement is zero, and as initial stripe in Eq. (7) the pixels along Δz=0 (along the rotation axis) have been selected. Fig. 13(b) shows the Δz displacement maps obtained with FP, and Fig. 13(c) the corresponding Δz displacement profiles (along the middle x_2 axis) which is compared with a linear fitting. A good coincidence is obtained with a mean root mean square of their differences of 0.183 mm, a mean norm of residuals of 3.342

mm and a R square of 0.9999. From the fitted lines the actual rotated angles are obtained from their slope which are also shown on the figure.

The Δx displacement obtained using FP+2D-DIC with the proposed speckle image distortion method again coincides with the Δx displacements obtained using Eq. (16) with Ncorr software for surfaces rotated below 55º. Fig. 13(d) shows the corresponding Δx values along the x_1-profiles (of pixels from the reference images). A very good coincidence is obtained with a mean root mean square of 0.027 mm, mean norm of residuals of 0.573 mm and a mean R square of 1. It is important to remark that with Ncorr it was not possible to correctly process the rotated surface of 55º and 60º because of the too large speckle distortion produced by these rotations. When these results are compared with those obtained with 3D-DIC, also a good coincidence is obtained with a mean root mean square of their differences of 0.137 mm, mean norm of residuals of 2.723 mm and a mean R square of 0.9995.

The data and the MATLAB (version R2018a) programs used to obtain the presented results can be downloaded from [dataset] [12]. The algorithms in this open access are not compiled, allowing their handling and understanding. But this makes their processing time much longer than if they were compiled.

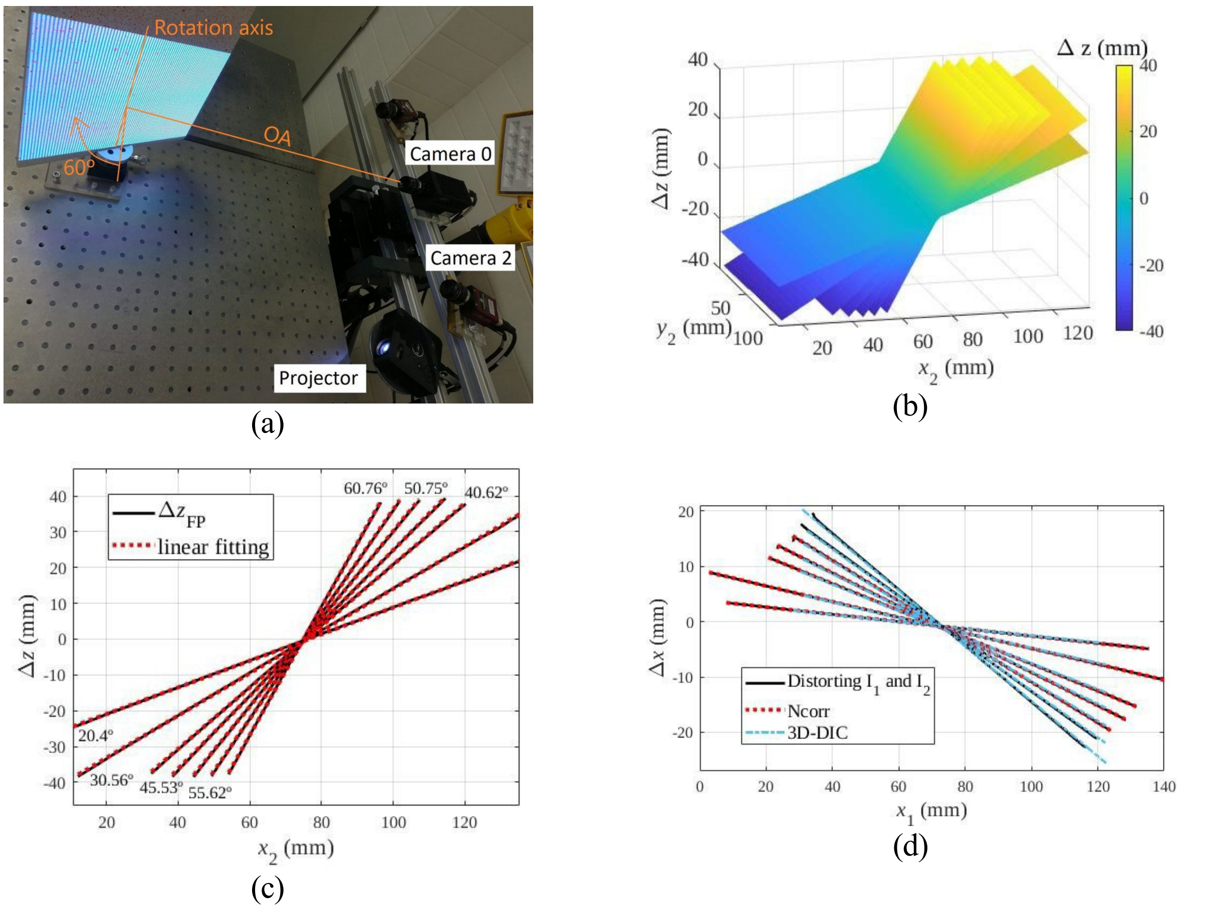

Fig. 13. (a) Experimental set-up for measuring the 3D displacements of the surface elements of a plane that is rotated between 20º and 60º. (b) Δz maps obtained with FP, (c) x_2-profiles of the Δz maps with linear fitting. (d) Δx displacement along x_1-profiles.

6 Conclusions

The proposed procedure to compute the in-plane displacement maps in DIC by distorting the speckle image of the reference and deformed surfaces using information of the out-of-plane displacement map, has demonstrated to be a powerful alternative, specially when the speckle images have experimented large deformations as a consequence of large out-of-plane displacements. For this proposal, an analytical equation has been derived to determine the in-plane displacements from the slope of the deformed specimens surface. With the proposed procedure, it is not necessary to perform the costly computational nonlinear minimization approach commonly used to determine subpixel displacements of the subsets. In particular, out-of-plane rotations of the reference plane of 55º and 60º could not be correctly processed with the Gauss-Newton iterative optimization scheme used in Ncorr software, but it was possible with the proposed procedure. For the other experiments, there were very good coincidence in the determination of the in-plane displacements, with a root mean square of their difference of about 0.03 mm (which is about $L/7$, or 1/7 the size of the image of a pixel). The validation of the measurements using a commercial 3D-DIC software, VIC-3D, was not possible due to possible errors of the 3D-DIC results attributed to a too small pan angle between cameras. However, a reasonable coincidence was obtained for the in-plane displacements, with a maximum difference of 1.5 mm (about 7% error) for the experiment where the plate was buckling, and a root mean square error of 0.137 mm (about 1/2 the size of the image of the pixel) for the experiment where the reference surface was rotated.

Appendix

As shown in Fig. 14, the subset within $\mathbf{I}_m$ of pixels around the location (x_m, y_m) used to calculate the intensity distribution of the corresponding pixel (x_2, y_2) in $\mathbf{I}_2$, is $(a{:}a+v-1,\ b{:}b+v-1)$ being

$$a = \begin{cases} \text{round}(x_m) - v/4 & \text{if } x_m \geqslant \text{round}(x_m), \\ \text{round}(x_m) - v/4 - 1 & \text{if } x_m < \text{round}(x_m). \end{cases} \tag{A.1}$$

the same for b but considering y_m. The location of the maximum of the intensity within this subset is at

$$(x_C, y_C) = (x_m - (a - v/8),\ y_m - (b - v/8)). \tag{A.2}$$

This subset is updated with the intensity values of a subset of the same site whose pixel values are the intensity values of a Gaussian function centered at (x_C, y_C) and with total intensity values normalized to the value of $\mathbf{I}_2(x_2, y_2)$. As standard deviation half pixel size is used.

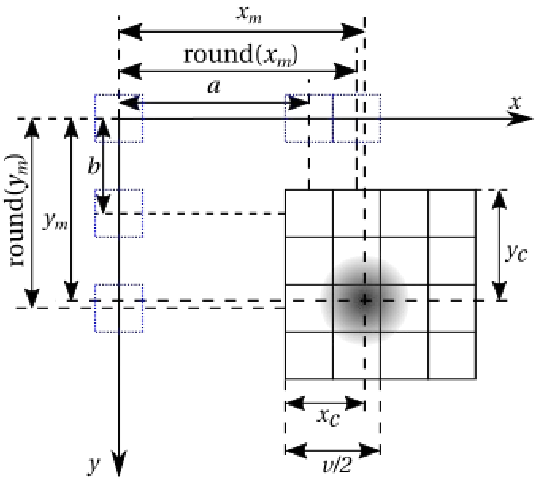

Fig. 14. Scheme for generating a distorted speckle image by translating pixel intensities to a new position.

Bibliography

[1] Sutton MA, Orteu JJ, Schreier HW, Image Correlation for Shape, Motion and Deformation Measurements. New York, USA: Springer; 2009.

[2] Dong B, Zeng F, Pan B, A Simple and Practical Single-Camera Stereo-Digital Image Correlation Using a Color Camera and X-Cube Prism, Sensors 2019; 19(21): 4726.

[3] Zhong FQ, Shao XX, Quan C, 3D digital image correlation using a single 3CCD colour camera and dichroic filter. Meas Sci Technol 2018; 29(4): 045401.

[4] Blaber J, Adair B, Antoniou A. Ncorr: Open-Source 2D Digital Image Correlation Matlab Software. Exp Mech 2015; 55(6): 1105–1122.

[5] Pan B. Reliability-guided digital image correlation for image deformation measurement. Opt Soc of Am 2009; 48(8): 1535-1542.

[6] Zhong F., Quan C. Digital image correlation in polar coordinate robust to a large rotation. Opt Lasers Eng 2017; 98: 153-158.

[7] Felipe-Sesé L, Siegmann P, Díaz-Garrido F, Patterson EA. Simultaneous in- and out-of-plane displacement measurements using fringe projection and digital image correlation. Opt Lasers Eng 2014; 52: 66–74.

[8] Felipe-Sese L, Siegmann P, Diaz-Garrido F, Patterson EA. Integrating fringe projection and digital image correlation for high quality measurements of shape changes. Opt Eng 2014; 53(4): 044106.

[9] Siegmann P, Felipe-Sese L, Diaz-Garrido F. Improved 3D displacement measurements method and calibration of a combined fringe projection and 2D-DIC system. Opt Lasers Eng 2017; 88: 255–264.

[10] Gmez-Pedrero JA, Quiroga JA, Servn M. Adaptive asynchronous algorithm for fringe pattern demodulation. Appl Opt 2008;47(21):3954–60.

[11] Hung PC, Voloshin AS. In-plane Strain Measurement by Digital Image Correlation. J of the Braz Soc of Mech Sci & Eng 2003; XXV(3): 215-221.

[dataset][12] Siegmann P. DIC with speckle distortion, v1; 2019. http://agamenon.tsc.uah.es/Personales/philip/pagina_files/software_philip.html